

# Selective Cell Penetrating Peptide-Functionalized Envelope-Type Chimeric Lipopepsomes Boost Systemic RNAi Therapy for Lung Tumors

Min Qiu, Jia Ouyang, Yaohua Wei, Jian Zhang, Qing Lan, Chao Deng,\*  
and Zhiyuan Zhong\*

Small interfering RNA (siRNA) is considered a highly specific and potent biotherapeutic that holds tremendous potential for the treatment of various diseases. The clinical translation of siRNA is, however, greatly impeded by the lack of safe and efficient delivery vehicles *in vivo*. Here, the development of selective cell penetrating peptide (CPP33)-functionalized chimeric lipopepsomes (CPP33-CLP) for efficient encapsulation and selective delivery of polo-like kinase 1 specific siRNA (siPLK1) to orthotopic A549 human lung tumor *in vivo* is reported. Interestingly, siRNA is tightly encapsulated into CPP33-CLP with a superb encapsulation efficiency of over 95% owing to the thick strong electrostatic interactions. Notably, siPLK1-loaded CPP33-CLP (siPLK1-CPP33-CLP) is selectively internalized by A549 human lung cancer cells, efficiently escapes from endosomes, and swiftly releases siRNA into the cytoplasm, affording a significant sequence-specific gene silencing *in vitro*. Moreover, siPLK1-CPP33-CLP exhibits prolonged blood circulation, enhanced tumor accumulation, effective suppression of tumor growth, and considerably elevated survival time of orthotopic A549 human lung tumor-bearing nude mice. These chimeric lipopepsomes appear as an attractive and potent nanoplatform for safe and targeted siRNA delivery.

## 1. Introduction


RNA interference (RNAi) mediated by small interfering RNA (siRNA) has shown significant potential for personalized therapy of various intractable diseases, including cancer, viral

infections, and autoimmune diseases.<sup>[1]</sup> The clinical translation of RNAi in cancer therapy is nevertheless hindered by their intrinsic susceptibility to enzymatic degradation, unsatisfactory plasma life *in vivo*, and inferior cellular uptake and endosomal escape.<sup>[2]</sup> To this end, different nanoplatforms fabricated from cationic polymers,<sup>[3]</sup> lipids,<sup>[4]</sup> peptides,<sup>[2c,5]</sup> inorganic materials,<sup>[6]</sup> and inorganic/polymer hybrids<sup>[7]</sup> have been broadly exploited for siRNA delivery. Among them, synthetic polypeptides are one of the most promising materials for siRNA delivery owing to their outstanding biocompatibility, *in vivo* degradability, and exclusive hierarchical structure.<sup>[8]</sup> Kataoka and coworkers reported that polyion complex (PIC) micelles based on poly(ethylene glycol)-poly(L-lysine) (PEG-PLL) and PEG-poly(L-aspartamide) diblock copolymers were able to systemically deliver siRNA to subcutaneous HeLa cervical and A549 lung tumor models.<sup>[9]</sup> The stability

of PIC micelles could be improved by incorporating another hydrophobic block such as poly(L-aspartamide) bearing a hydrophobic dimethoxynitrobenzyl ester moiety and poly(L-leucine) into the core<sup>[10]</sup> or cross-linking the core using a cross-linker.<sup>[11]</sup> Cheng and Yin reported on a fascinating cationic helical polypeptide, poly( $\gamma$ -(4-((2-(piperidin-1-yl)ethyl)aminomethyl)benzyl)-L-glutamate) (PPABLG), which could facilitate direct translocation and endosomal escape of siRNA via the formation of pores on cellular and endosomal membranes.<sup>[12]</sup> Tumor necrosis factor  $\alpha$  (TNF- $\alpha$ ) siRNA/PPABLG complexes exhibited effective downregulation of TNF- $\alpha$  and anti-inflammatory effect in mice bearing hepatic sepsis. Like most cationic systems, cationic polypeptides encounter issues like low stability and lack of specificity *in vivo* that make them less effective for systemic RNAi therapy.<sup>[13]</sup> Recently, envelope-type nanovehicles consisting of a complexed nucleic acid core and a polymer/lipid envelope structure modified with functional molecules showed interesting properties, including improved nucleic acid packing, high stability against enzymes, and versatile functionalization.<sup>[3c,14]</sup> In particular, chimeric polymersomes formed from asymmetric ABC triblock copolymers have appeared to be an ideal envelope-type carrier for biopharmaceuticals including

Dr. M. Qiu, Y. H. Wei, Dr. J. Zhang, Prof. C. Deng, Prof. Z. Y. Zhong  
Biomedical Polymers Laboratory  
Jiangsu Key Laboratory of Advanced Functional Polymer  
Design and Application  
College of Chemistry  
Chemical Engineering and Materials Science  
and State Key Laboratory of Radiation Medicine and Protection  
Soochow University  
Suzhou 215123, China  
E-mail: cdeng@suda.edu.cn; zyzhong@suda.edu.cn

Dr. J. Ouyang, Prof. Q. Lan  
Department of Neurosurgery  
The Second Affiliated Hospital of Soochow University  
Suzhou 215123, China

 The ORCID identification number(s) for the author(s) of this article can be found under <https://doi.org/10.1002/adhm.201900500>.

DOI: 10.1002/adhm.201900500

proteins and siRNA, providing superior loading, high in vivo stability, and enhanced therapeutic efficacy.<sup>[15]</sup> In chimeric polymericosomes, the polyelectrolytes such as polyethylenimine (C block) are shorter than PEG (A block), which renders polyelectrolytes mostly located in the aqueous lumen, thereby achieving high loading of siRNA via electrostatic interactions, while PEG at the outer surface, thereby guaranteeing good biocompatibility and long circulation time. The use of short polyethylenimine might, however, induce toxicity concerns and tedious preparation process.<sup>[16]</sup>

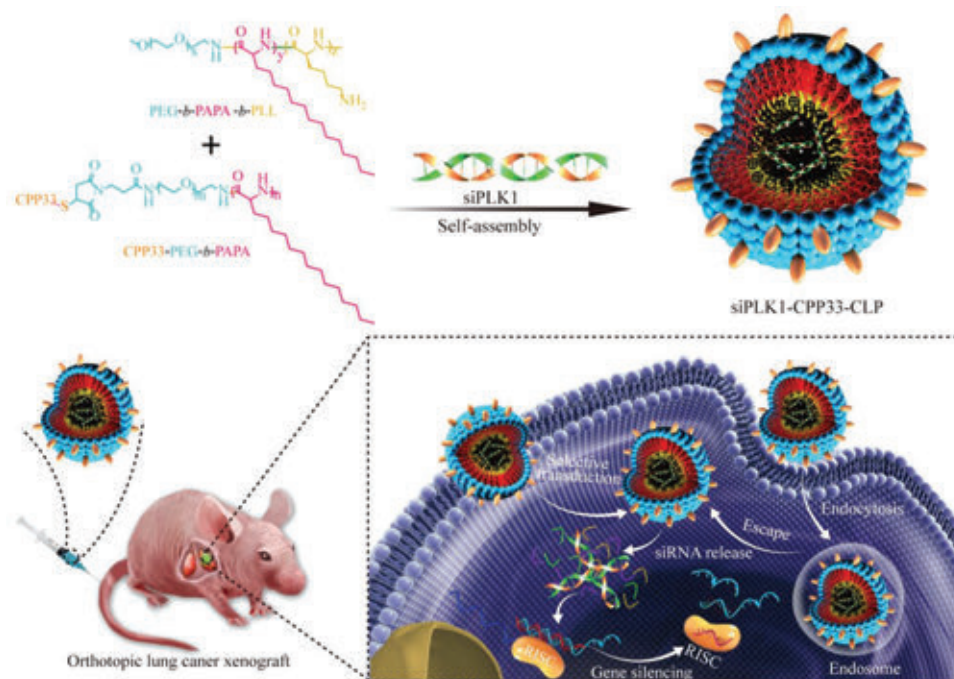
Herein, we report facile construction of chimeric lipopepsomes from poly(ethylene glycol)-*b*-poly( $\alpha$ -aminopalmitic acid)-*b*-poly(L-lysine) (PEG-*b*-PAPA-*b*-PLL) asymmetric triblock copolymer as an envelope-type carrier for efficient delivery of polo-like kinase 1 siRNA (siPLK1) to orthotopic human lung tumor xenografts in vivo (Scheme 1). PLL was devised shorter than PEG, to efficiently load siRNA into the watery lumen. The PAPA segments in the membrane would present strong lipid-lipid packing, which might not only afford high stability as previously reported for different systems,<sup>[17]</sup> but also protect siRNA from degradation. The surface was further functionalized with lung cancer-specific cell penetrating peptide CPP33 (RLWMR-WYSPRTRAYGC), which has demonstrated a high specificity and cell penetrating effect to A549 human lung cancer cells.<sup>[18]</sup> PLK1 is an endogenous cell cycle kinase. The silencing of PLK1 in cancer cells would result in cell cycle arrest, apoptosis, and “mitotic catastrophe.”<sup>[19]</sup> siPLK1 has been reported to effectively retard the growth of different cancer cells.<sup>[20]</sup> The results reveal that this envelope-type vehicle achieves high loading and efficient systemic delivery of siPLK1 in orthotopic A549 lung

tumor xenografts, affording significant suppression of tumor progression and elevated survival rate.

## 2. Results and Discussion

### 2.1. Fabrication of CPP33-Functionalized Chimeric Lipopepsomes and siRNA Loading

CPP33-functionalized chimeric lipopepsomes (CPP33-CLP) were co-self-assembled from PEG-*b*-PAPA-*b*-PLL triblock copolymer ( $M_n = 5.0\text{--}10.8\text{--}1.9 \text{ kg mol}^{-1}$ ) and CPP33-modified PEG-*b*-PAPA diblock copolymer (CPP33-PEG-*b*-PAPA,  $M_n = 6.0\text{--}10.0 \text{ kg mol}^{-1}$ ). The PEG chain in CPP33-PEG-*b*-PAPA was designed longer than that of PEG-*b*-PAPA-*b*-PLL to maximize exposure of CPP33 peptide on the outer surface of lipopepsomes. Asymmetric PEG-*b*-PAPA-*b*-PLL copolymer was readily acquired by sequential ring-opening polymerization (ROP) of  $\alpha$ -aminopalmitic acid *N*-carboxyanhydride (APA-NCA) and  $\epsilon$ -benzyloxycarbonyl-L-lysine *N*-carboxyanhydride (ZLL-NCA) using PEG-NH<sub>2</sub> as a macroinitiator, followed by deprotection of benzyloxycarbonyl groups (Scheme S1, Supporting Information). The structure of PEG-*b*-PAPA-*b*-PLL was verified by characteristic signals of PEG ( $\delta$  3.73 and 3.48), PAPA ( $\delta$  1.66, 1.24, and 0.87), and PZLL ( $\delta$  7.29, 5.07, and 3.07) as shown in Figure S1 (Supporting Information). By comparing the signal integrals at  $\delta$  0.87 (methyl protons of PAPA) and  $\delta$  5.07 (methylene protons of PZLL) to  $\delta$  3.73 (methylene protons of PEG), the degree of polymerization (DP) of PAPA and PZLL was readily acquired to be 40 and 15, respectively (Table S1,



**Scheme 1.** Illustration of CPP33-CLP for efficient loading and selective delivery of siRNA to orthotopic A549 human lung tumor. siPLK1-encapsulated CPP33-CLP exhibits prolonged blood circulation, enhanced tumor accumulation and selectivity, effective tumor growth inhibition, and considerably elevated survival time of orthotopic A549 lung tumor-bearing mice.

Supporting Information). PEG-*b*-PAPA-*b*-PZLL was deprotected with HBr/CF<sub>3</sub>COOH. The resulting copolymer, PEG-*b*-PAPA-*b*-PLL, was isolated by precipitation in excess diethyl ether. To remove homopolymers like PEG and PLL if present, PEG-*b*-PAPA-*b*-PLL was redissolved in tetrahydrofuran (THF) and exhaustively dialyzed against deionized (DI) water (MWCO = 7000 Da). PEG-*b*-PAPA-*b*-PLL was freeze-dried and acquired as white powder. <sup>1</sup>H NMR spectrum of PEG-*b*-PAPA-*b*-PLL exhibited that signals at δ 7.29 and 5.07 derived from the benzyloxycarbonyl protection group disappeared (Figure S2, Supporting Information), confirming complete deprotection. The DPs of PAPA and PLL blocks were similar to those of PAPA and PZLL in the parent PEG-*b*-PAPA-*b*-PZLL copolymer, indicating that polypeptide is intact during deprotection. CPP33-PEG-*b*-PAPA copolylopolypeptide was acquired by polymerization of APA-NCA using maleimide (Mal)-PEG-NH<sub>2</sub> followed by Michael-type addition reaction with thiol-containing CPP33 peptide (Scheme S2, Supporting Information). <sup>1</sup>H NMR spectrum indicated that Mal-PEG-*b*-PAPA possessed prescribed *M<sub>n</sub>* (Figure S3 and Table S1, Supporting Information). The structure of CPP33-PEG-*b*-PAPA was verified by the appearance of CPP33 resonances at δ 6.97 (Figure S4, Supporting Information). The degree of CPP33 conjugation was calculated to be 87%, by detecting the arginine amount using 9,10-phenanthrene-quinone method.<sup>[21]</sup>

CPP33-CLP exhibited a small size of ~90 nm, a narrow polydispersity index, and a distinct vesicular structure (Figure 1a). The size of lipopepsomes displayed in transmission electron microscopy (TEM) image was smaller than that determined by differential light scattering (DLS), which is likely due to the shrinking of lipopepsomes upon drying. Following 12 h incubation against 10% fetal bovine serum (FBS), CPP33-CLP exhibited negligible size change, signifying their robust structure (Figure S5, Supporting Information). siRNA-loaded CPP33-CLP (siRNA-CPP33-CLP) was fabricated from 80 mol% PEG-*b*-PAPA-*b*-PLL and 20 mol% CPP33-PEG-*b*-PAPA. We have shown that polymersomes with 20 mol% CPP33 exhibited optimal targetability toward A549 lung cancer cells.<sup>[18b]</sup> Interestingly, CPP33-CLP showed efficient encapsulation of siRNA with a high encapsulation efficiency of >95% (Table S2, Supporting Information). siRNA-CPP33-CLP was observed to have a close to neutral surface charge, corroborating that positively charged PLL segment is preferentially located in the lumen. The high siRNA loading is due to charge interaction between siRNA and PLL in the inner lumen. The gel retardation studies showed that siRNA was tightly encapsulated into CPP33-CLP and siRNA-CPP33-CLP was stable following 17 h incubation against 10% FBS (Figure 1b), suggesting a high stability of siRNA-CPP33-CLP.

## 2.2. Cellular Uptake, Endosomal Escape, and Gene Silencing Efficacy

We next investigated the cellular uptake and intracellular trafficking behaviors of CPP33-CLP using flow cytometry and confocal laser scanning microscopy. As shown in Figure 1c, CPP33 functionalization clearly boosted the cellular uptake of CLP into A549 cells. To study its cell specificity, we compared the cellular

uptake of CPP33-CLP in different cells. The results showed that A549 human lung cancer cells had significantly higher cellular uptake of CPP33-CLP than other cancer cells including MDA-MB-231 human breast cancer and SMMC-7721 human hepatocellular carcinoma as well as mouse brain microendothelial cell lines (Figure 1d), supporting high specificity of CPP33 to A549 lung cancer cells.<sup>[18a,b,22]</sup>

To unveil the uptake mechanism of CPP33-CLP, A549 cells were pretreated with different endocytic inhibitors such as chlorpromazine, dynasore, amiloride hydrochloride, and methyl-β-cyclodextrin (MβCD). Flow cytometry demonstrated that chlorpromazine, amiloride hydrochloride, and MβCD did not prevent cell entry, while dynasore significantly blocked the uptake of CPP33-CLP into the A549 cells (Figure 1e), indicating that CPP33 facilitates A549 cell internalization of CLP via a dynamin-dependent and clathrin/micropinositosis/caveolae-independent pathway, similar to previous observation for poly(ethylene glycol)-*b*-poly(trimethylene carbonate-co-dithiolane trimethylene carbonate)-*b*-poly(ethyleneimine) polymersomes systems.<sup>[18b]</sup> Endosomal entrapment is one of the key challenges that greatly reduce the efficacy of siRNA formulations.<sup>[2a,23]</sup> To investigate its endosomal escape behavior, CPP33-CLP was loaded with Cy5-labeled siPLK1 and endosomes were stained with LysoTracker Blue. As shown in Figure 1f, more red dots (Cy5-siPLK1) were observed in cells treated with Cy5-siPLK1-CPP33-CLP than those with Cy5-siPLK1-CLP, indicating that CPP33 facilitates the endosomal escape of siRNA. Quantitative real-time polymerase chain reaction (qRT-PCR) was carried out to explore the specific gene silencing effect of siPLK1-CPP33-CLP in A549 cancer cells. As shown in Figure 1g, siPLK1-CLP displayed effective gene silencing efficacy and cells treated with siPLK1-CLP exhibited decreasing PLK1 mRNA level with increasing siRNA concentration from 200 × 10<sup>-9</sup> to 400 × 10<sup>-9</sup> M. Moreover, siPLK1-CPP33-CLP exhibited significantly better PLK1 gene silencing efficacy than siPLK1-CLP, whereas siScramble-CPP33-CLP led to little silencing of PLK1 mRNA. Western blot analysis confirmed that both siPLK1-CLP and siPLK1-CPP33-CLP could efficiently downregulate the expression of PLK1 protein (Figure 1h). The potent gene silencing of siPLK1-CPP33-CLP might be attributed to its high uptake by A549 cells and fast endosomal escape.

## 2.3. In Vivo Pharmacokinetics and Biodistribution of siPLK1-CPP33-CLP

The pharmacokinetic studies in healthy Balb/c mice followed by a single injection of Cy5-siPLK1-loaded lipopepsomes via tail vein showed that both Cy5-siPLK1-CPP33-CLP and Cy5-siPLK1-CLP presented a prolonged blood circulation time with an elimination half-life (*t*<sub>1/2,β</sub>) of 3.4 and 2.9 h, respectively (Figure 2a). On the contrary, naked Cy5-siPLK1 was swiftly eliminated following systemic injection (*t*<sub>1/2,β</sub> = 0.14 h). Cy5-siPLK1-CPP33-CLP revealed a 12.2-fold higher area under curve than naked Cy5-siPLK1. In comparison, siRNA polyplexes are prone to disassembly and rapid elimination from the body with a short *t*<sub>1/2,β</sub> of less than 30 min.<sup>[24]</sup> To visualize its targetability in vivo, CPP33-CLP was labeled with Cy5 and i.v. administered to subcutaneous A549 tumor-bearing nude



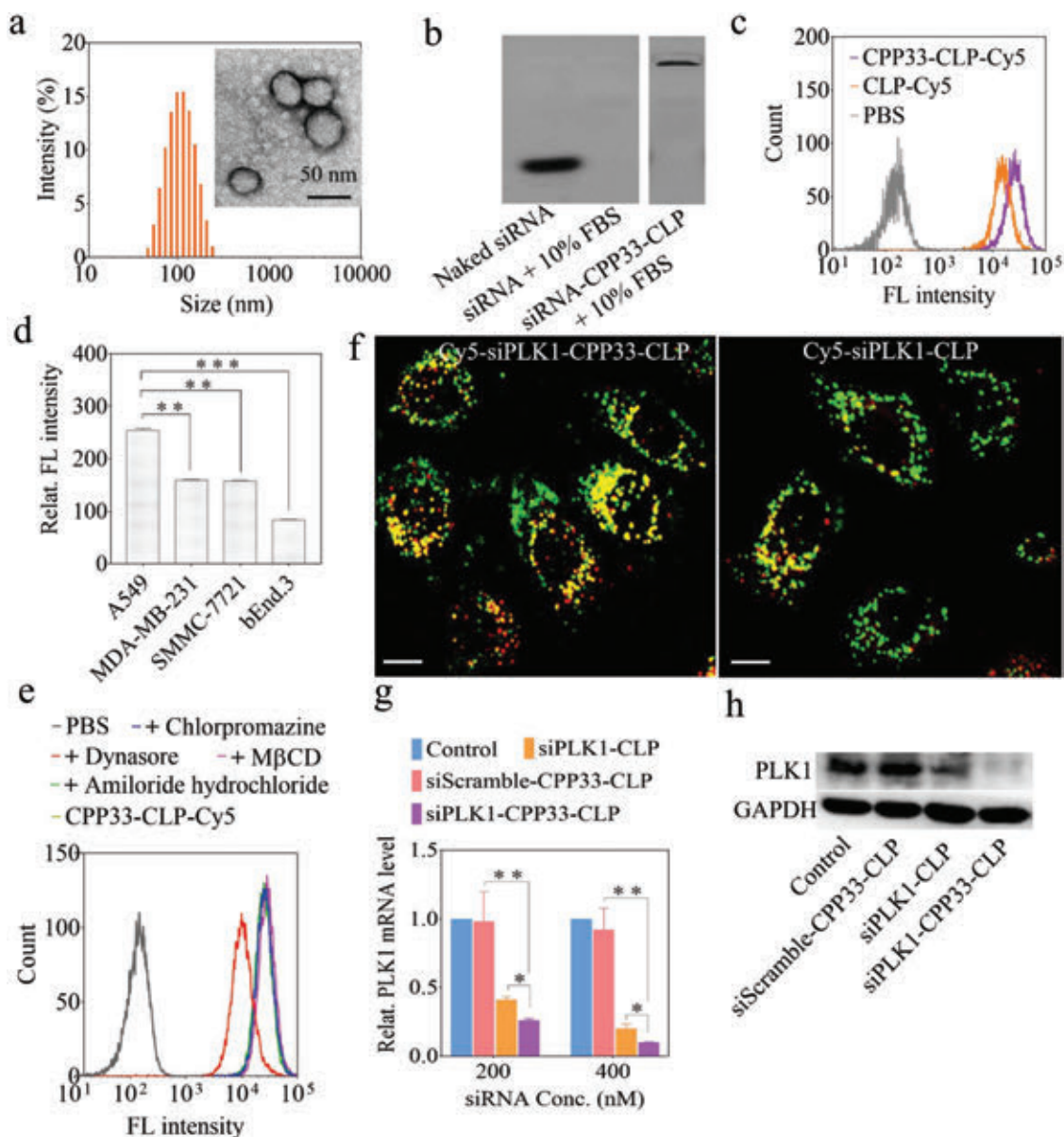


**Figure 1.** a) Size distribution of CPP33-CLP determined by DLS. Inset is the TEM image of CPP33-CLP. b) Gel retardation assays of siPLK1-CPP33-CLP treated with or without 10% FBS for 17 h. c) Flow cytometry of A549 cells treated with CPP33-CLP-Cy5 for 2 h (Cy5 concentration:  $2 \times 10^{-9}$  M). d) Cellular uptake of CPP33-CLP-Cy5 for different cells using flow cytometry at 2 h incubation with CPP33-CLP-Cy5 (Cy5 concentration:  $2 \times 10^{-9}$  M). e) Uptake mechanisms of CPP33-CLP studied by flow cytometry following 2 h incubation with CPP33-CLP-Cy5. Cells were pretreated with amiloride hydrochloride ( $100 \times 10^{-6}$  M), chlorpromazine ( $100 \times 10^{-6}$  M), dynasore ( $80 \times 10^{-6}$  M), and M $\beta$ CD ( $7.6 \times 10^{-3}$  M) for 30 min. f) Endosomal escape behavior of Cy5-siPLK1-CPP33-CLP in A549 cells observed by confocal microscopy following 2 h incubation with Cy5-siPLK1-CPP33-CLP and Cy5-siPLK1-CLP (Cy5-siPLK1 concentration:  $200 \times 10^{-9}$  M), and another 2 h in fresh medium. Endosomes were stained with LysoTracker Blue (for better read we give them green false color) and Cy5-siPLK1 were colored red. Scale bar: 10  $\mu$ m. Gene silencing effect of siPLK1-CPP33-CLP in A549 cells characterized by g) qRT-PCR and h) Western blot. The cells following the treatment with different formulations for 4 h were cultured in fresh media for another 44 h (siRNA concentration:  $200 \times 10^{-9}$  or  $400 \times 10^{-9}$  M). Data are presented as mean  $\pm$  SD ( $n = 4$ , \* $P < 0.05$ , \*\* $P < 0.01$ , \*\*\* $P < 0.001$ ).

mice. Of note, intense Cy5 fluorescence was visualized in the tumor area at 6 h postinjection of Cy5-labeled CPP33-CLP (CPP33-CLP-Cy5), in sharp contrast with the much weaker fluorescence in mice treated with Cy5-labeled CLP (CLP-Cy5) (Figure 2b). The ex vivo images showed that CPP33-CLP-Cy5 gave much stronger fluorescence intensity than nontargeting CLP-Cy5 in the tumor tissue at 48 h postinjection (Figure 2c). The biodistribution of Cy5-siPLK1-CPP33-CLP in orthotopic

A549 tumor-bearing nude mice was quantified at 6 h postinjection of Cy5-siPLK1-CPP33-CLP. As shown in Figure 2d, Cy5-siPLK1-CPP33-CLP exhibited an improved Cy5-siRNA tumor accumulation of 3.14% injected dose per gram of tissue ( $\text{ID g}^{-1}$ ), which was about 1.9-fold higher than that of Cy5-siPLK1-CLP ( $1.69\% \text{ ID g}^{-1}$ ), confirming that CPP33 peptide facilitates tumor accumulation and retention of siRNA-loaded lipopepsomes. Of note, both Cy5-siPLK1-CPP33-CLP and Cy5-siPLK1-CLP

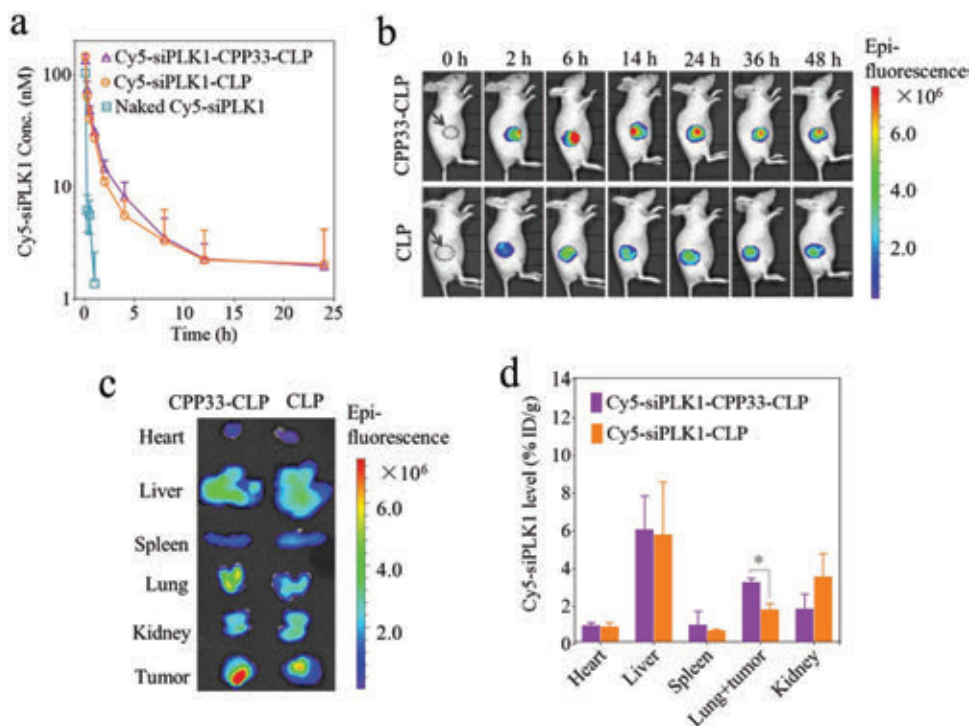


**Figure 2.** a) In vivo pharmacokinetics of Cy5-siPLK1-CPP33-CLP, Cy5-siPLK1-CLP, and naked Cy5-siPLK1 in healthy Balb/c mice. b) In vivo imaging of subcutaneous A549 tumor-bearing mice following i.v. administration with CPP33-CLP-Cy5 or CLP-Cy5. c) Ex vivo images of main organs and tumors from subcutaneous A549 tumor-bearing mice treated with CPP33-CLP-Cy5 and CLP-Cy5 at 48 h. d) Biodistribution of Cy5-siPLK1-CPP33-CLP and Cy5-siPLK1-CLP in main organs and tumors of orthotopic A549 tumor-bearing mice at 6 h postinjection ( $n = 3$ ,  $*P < 0.05$ ,  $**P < 0.01$ ,  $***P < 0.001$ ).

exhibited a high accumulation in the liver, likely due to uptake by the mononuclear phagocytic system, as reported for most nanoparticulate systems.<sup>[25]</sup>

#### 2.4. In Vivo Antitumor Activity of siPLK1-CPP33-CLP

The in vivo antitumor activity of siPLK1-CPP33-CLP was evaluated using orthotopic A549-Luc human lung cancer tumor xenografts. PLK1 overexpressed in a broad spectrum of human tumors has been viewed as a potential therapeutic target in various cancers.<sup>[19b]</sup> siPLK1-CPP33-CLP, CPP33-CLP, or siScramble-CPP33-CLP was intravenously administered via tail vein at a dosage of 150 nmol siPLK1 equiv.  $\text{kg}^{-1}$  every other day (four injections in total). Luciferase imaging was employed to track the tumor progression. **Figure 3a** shows that siPLK1-CPP33-CLP effectively inhibited tumor growth. The semi-quantification of the bioluminescence on day 12 showed that mice treated with siPLK1-CPP33-CLP had about 1.9-fold and 4.8-fold lower photon flux in the lungs than those with siPLK1-CLP and siScramble-CPP33-CLP, respectively (Figure 3b). The lung photographs of different treatment groups collected at day 12 revealed that siPLK1-CPP33-CLP had evidently lower tumor burden than the controls, confirming its better therapeutic efficacy (Figure S6, Supporting Information). The survival curves revealed that mice administered with siPLK1-CPP33-CLP had an elevated survival rate with a median survival time of 45 days, which was remarkably longer than those treated with siPLK1-CLP (36 days) and

siScramble-CPP33-CLP (26 days) (Figure 3c). Importantly, the siPLK1-CPP33-CLP group led to negligible body weight loss (Figure 3d), demonstrating its low systemic toxicity and effective inhibition of tumor invasion. Of note, mice treated with siPLK1-CPP33-CLP presented well-organized lung structure, while large areas of proliferating tumor cells were noticed in the lung of mice administered with siScramble-CPP33-CLP and PBS (Figure S7, Supporting Information). It is evident, therefore, that siPLK1-CPP33-CLP enables safe and efficient delivery of siRNA to orthotopic lung tumors in vivo.

### 3. Conclusions

We show here rationally designed chimeric lipopepsomes based on poly(ethylene glycol)-*b*-poly( $\alpha$ -aminopalmitic acid)-*b*-poly(L-lysine) as an envelope-type nanovehicle for efficient encapsulation and tumor-targeted delivery of siRNA in vivo. siPLK1-CPP33-CLP mediates effective sequence-specific in vitro gene silencing in A549 human lung cancer cells, and achieves significantly enhanced tumor suppression and improved survival time of nude mice bearing orthotopic lung tumor xenografts. siPLK1-CPP33-CLP exhibits several exclusive advantages for siRNA therapy: 1) PEG-*b*-PAPA-*b*-PLL triblock copolymer can be readily acquired with controlled molecular weight and high yield through NCA polymerization followed by acid deprotection; 2) siRNA can be efficiently encapsulated into the watery lumen of chimeric lipopepsomes via charge complexation between siRNA and PLL segment; 3) robust

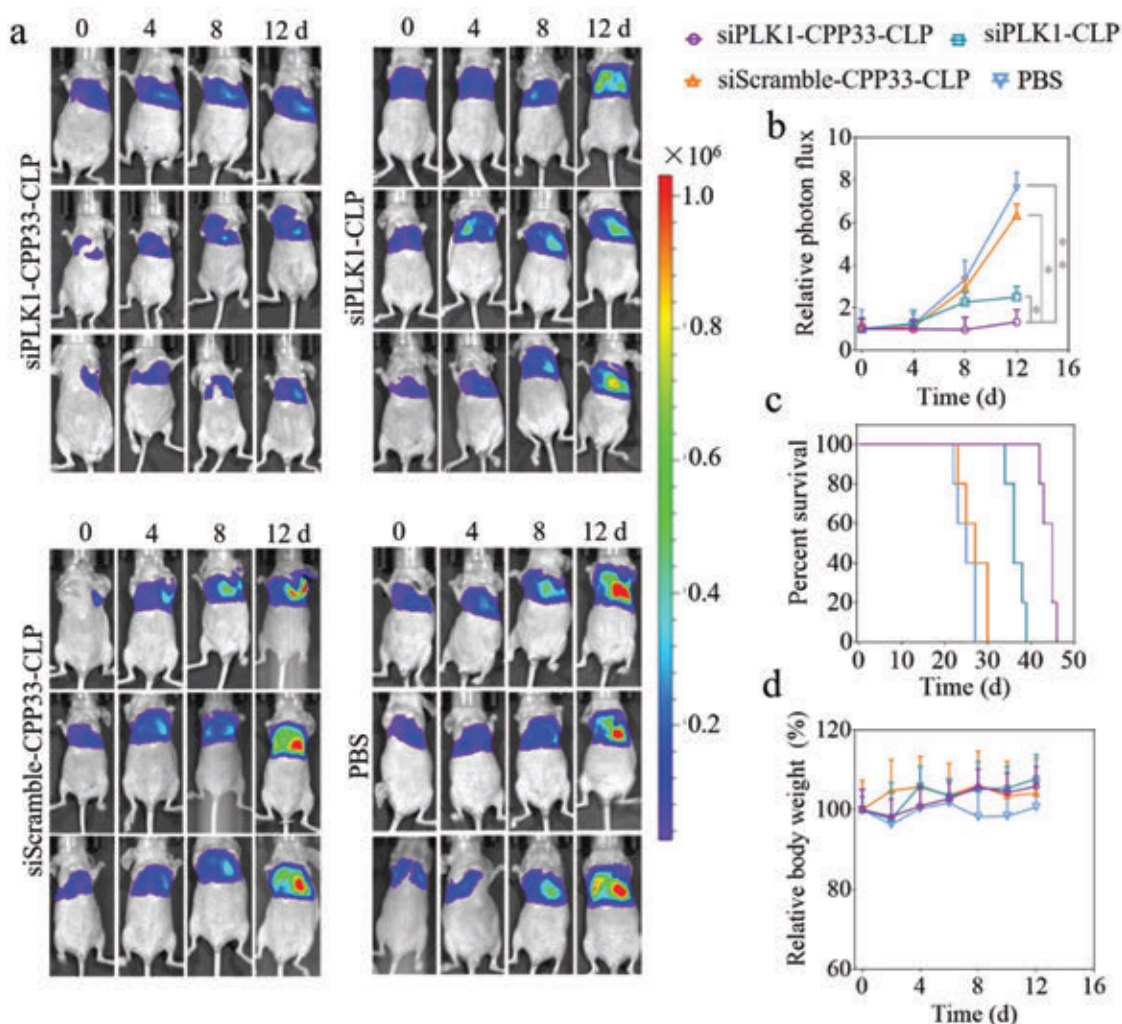


**Figure 3.** a) Luminescence optical images of orthotopic A549-Luc lung tumor-bearing nude mice treated with siPLK1-CPP33-CLP, siPLK1-CLP, siScramble-CPP33-CLP, or PBS. The formulations were administrated on days 0, 2, 4, and 6 (dosage: 150 nmol siPLK1 equiv. kg<sup>-1</sup>). b) Average A549-Luc tumor luminescence levels of lungs in tumor-bearing mice following different treatments in 12 days ( $n = 5$ ,  $*P < 0.05$ ,  $**P < 0.01$ ,  $***P < 0.001$ ). c) Kaplan–Meier survival curves of mice. Statistical analysis: siPLK1-CPP33-CLP versus siPLK1-CLP, siScramble-CPP33-CLP, or PBS,  $P < 0.01$ ; siPLK1-CLP versus siScramble-CLP or PBS,  $P < 0.01$  (Kaplan–Meier analysis, log-rank test). d) Body weight changes of mice within 12 days.

membrane of lipopepsomes allows good protection of siRNA from degradation in vivo; and 4) it can be selectively internalized by A549 human lung cancer cells as well as efficiently escape from endosomes and rapidly release siRNA into the cytoplasm, affording a remarkable sequence-specific suppression of cancer-associated PLK1 expression and A549 tumor progression. These envelope-type chimeric lipopepsomes provide a robust, safe, simple, and versatile nanoplatform for targeted systemic siRNA delivery.

#### 4. Experimental Section

**Preparation of PEG-*b*-PAPA-*b*-PLL and CPP33-PEG-*b*-PAPA Copolymers:** PEG-*b*-PAPA-*b*-PLL triblock copolymer was prepared by the sequential ROP of APA-NCA and ZLL-NCA monomers in the presence of PEG-NH<sub>2</sub>, followed by deprotection of benzyloxycarbonyl groups. Briefly, a solution of PEG-NH<sub>2</sub> (0.40 g, 0.08 mmol) in

dimethylformamide (DMF, 40 mL) was rapidly mixed with APA-NCA (1.04 g, 3.52 mmol) solution in DMF (15.0 mL). After stirring at 35 °C under N<sub>2</sub> for 72 h, ZLL-NCA (0.44 g, 1.44 mmol) solution in DMF (4.0 mL) was added and the mixture was stirred at 35 °C for another 72 h. The resulting PEG-*b*-PAPA-*b*-PZLL copolymer was isolated by precipitating in excess diethyl ether, and purified through redissolving in dichloromethane and precipitating in diethyl ether thrice. Yield: 83%. <sup>1</sup>H NMR (600 MHz, CDCl<sub>3</sub>/CF<sub>3</sub>COOH (9/1, v/v), Figure S1, Supporting Information,  $\delta$ ): 7.29 (–C<sub>6</sub>H<sub>5</sub>), 5.07 (C<sub>6</sub>H<sub>5</sub>CH<sub>2</sub>–), 4.48 (–COCHNH–), 3.73 (–OCH<sub>2</sub>CH<sub>2</sub>O–), 3.48 (–OCH<sub>3</sub>), 3.07 (–OCONHCH<sub>2</sub>–), 1.66 (–CH(NH)CH<sub>2</sub>CH<sub>2</sub>–), 1.24 (–CH<sub>2</sub>(CH<sub>2</sub>)<sub>12</sub>CH<sub>3</sub> and –CH(NH)CH<sub>2</sub>CH<sub>2</sub>CH<sub>2</sub>–), 0.87 (–CH<sub>2</sub>CH<sub>3</sub>).

For removal of benzyloxycarbonyl protection groups, HBr (33 wt% in HOAc, 0.19 mL, 1.0 mmol) was added to PEG-*b*-PAPA-*b*-PZLL (0.30 g, 0.015 mmol) solution in 3 mL CF<sub>3</sub>COOH. The reaction proceeded at 0 °C for 2 h, and the mixture was precipitated in excess diethyl ether. The resulting copolymer was redissolved in THF and exhaustively dialyzed against DI water (MWCO 7000 Da). PEG-*b*-PAPA-*b*-PLL was freeze-dried and acquired as white powder. Yield: 83%. <sup>1</sup>H NMR (600 MHz, CDCl<sub>3</sub>/CF<sub>3</sub>COOH (30/1, v/v), Figure S2, Supporting Information,  $\delta$ ):



4.49 (–COCHNH–), 3.74 (–OCH<sub>2</sub>CH<sub>2</sub>O–), 3.49 (–OCH<sub>3</sub>), 3.18 (–CH<sub>2</sub>NH<sub>2</sub>), 1.69 (–CH(NH)CH<sub>2</sub>CH<sub>2</sub>–), 1.47 (–CH<sub>2</sub>CH<sub>2</sub>CH<sub>2</sub>CH<sub>2</sub>NH<sub>2</sub>), 1.23 (–CH<sub>2</sub>(CH<sub>2</sub>)<sub>12</sub>CH<sub>3</sub> and –CH(NH)CH<sub>2</sub>CH<sub>2</sub>CH<sub>2</sub>–), 0.85 (–CH<sub>2</sub>CH<sub>3</sub>).

CPP33-PEG-*b*-PAPA was acquired through Michael addition reaction of CPP33 (RLWMRWYSPRTRAYGC) with Mal-PEG-*b*-PAPA that was similarly obtained by ROP of APA-NCA using Mal-PEG-NH<sub>2</sub> ( $M_n = 6.0 \text{ kg mol}^{-1}$ ). Briefly, a solution of Mal-PEG-*b*-PAPA (30 mg, 0.0018 mmol) was completely mixed with CPP33 solution (7.5 mg, 0.0035 mmol) under N<sub>2</sub>. The reaction was stirred at 30 °C for 12 h. The reaction mixture was dialyzed against DMF for 24 h to eliminate unreacted CPP33 and then against DI water for 48 h before lyophilization. Yield: 80%. The degree of CPP33 conjugation was obtained to be 87% by detecting the arginine amount using the 9,10-phenanthrene-quinone technique.

**Preparation of siRNA-Loaded Chimeric Lipopepsomes:** siRNA-CPP33-CLP were acquired using the solvent exchange technique. Typically, 100 μL of THF solution of 20 mol% CPP33-PEG-*b*-PAPA and 80 mol% mPEG-*b*-PAPA-*b*-PLL (polymer concentration: 5.0 mg mL<sup>−1</sup>) was mixed with 100 μL of siRNA in HEPES buffer (5 × 10<sup>−3</sup> M, pH 6.8). The mixture was then added dropwise to HEPES under stirring at room temperature (r.t.), followed by exhaustive dialysis (MWCO 350 kDa) against phosphate buffer (5 × 10<sup>−3</sup> M, pH 7.4). The amount of siRNA loaded into the lipopepsomes was determined by NanoDrop UV–vis spectrophotometer. The siRNA loading content (SLC) and efficiency (SLE) were determined using the following formulas:

$$\text{SLC (wt\%)} = (\text{weight of loaded siRNA} / \text{total weight of copolymer and siRNA}) \times 100 \quad (1)$$

$$\text{SLE (\%)} = (\text{weight of loaded siRNA} / \text{weight of siRNA in feed}) \times 100 \quad (2)$$

**In Vitro Gene Silencing Assays:** The in vitro gene silencing activities of siPLK1-CPP33-CLP were assessed by qRT-PCR and Western blot. For qRT-PCR, A549 cells were cultured in a six-well plate (1 × 10<sup>6</sup> cells per well) with RPMI-1640 media containing 10% v/v FBS, 1% v/v penicillin (100 IU mL<sup>−1</sup>), and streptomycin (100 μg mL<sup>−1</sup>) for 24 h. Then, siPLK1-CPP33-CLP, siPLK1-CLP, and siScramble-CPP33-CLP (siRNA concentration: 200 × 10<sup>−9</sup> and 400 × 10<sup>−9</sup> M) were added and incubated for 4 h. Then, the cells were incubated in fresh medium for another 44 h, and washed with PBS. Reverse transcription was carried out using SYBR Real-Time PCR kit (GenePharma, China) and quantitative PCR was performed by SYBR Real-Time PCR Assays Protocol with an ABI 7500 Fast Real-Time PCR System (Life Technologies, USA). Glyceraldehyde 3-phosphate dehydrogenase (GAPDH) was utilized as an endogenous housekeeping gene to normalize the PLK1 mRNA amount. The mRNA expression level was determined using comparative Ct method (2<sup>−ΔΔCt</sup>) with Life Technologies 7500 Software v2.0.

For Western blot analysis, equivalent protein determined using a bicinchoninic acid protein assay kit (Pierce/Thermo Scientific) was added to SDS-PAGE gels, separated by gel electrophoresis, and transferred to polyvinylidene difluoride membrane blocked with a solution of bovine serum albumin (5%) in Tris buffer. After incubating with PLK1 rabbit antibody (Cell Signaling) or GAPDH antibody (Cell Signaling) at 4 °C overnight, the expression of PLK1 was detected using horseradish peroxidase-conjugated secondary antibody at r.t. The signals were determined using SuperSignal ECL detection system (Pierce), and the bands were quantified using ImageJ software.

**In Vivo Antitumor Activity of siPLK1-CPP33-CLP:** The mice were handled under protocols approved by Soochow University Laboratory Animal Center and the Animal Care and Use Committee of Soochow University. In vivo antitumor activity of siPLK1-CPP33-CLP was evaluated using the orthotopic A549 lung cancer tumor model. The orthotopic A549-Luc xenograft tumor model was generated by injecting A549-Luc cells (1 × 10<sup>7</sup>) blended in 100 μL of PBS/Matrigel (4/1, v/v) into the left lung parenchyma of nude mice as per the previous report.<sup>[26]</sup> The mice were separated into four groups (six mice per group), and intravenously administrated with siPLK1-CPP33-CLP, siPLK1-CLP, or siScramble-CPP33-CLP at a dosage of 150 nmol siRNA equiv. kg<sup>−1</sup> every 2 days

(four doses in total). Mice were weighted and normalized to their initial weight on day 0. The tumor progression was examined by measuring the bioluminescence using IVIS Lumina II imaging system (Caliper Life Sciences) following the i.p. injection of D-luciferin potassium salt solution (15 mg mL<sup>−1</sup>, 100 μL) in PBS. On day 12, one mouse from each group was sacrificed and employed for histological evaluation.

**Statistical Analysis:** Data were expressed as mean ± standard deviation (SD). Difference between groups was assessed using the one-way analysis of variance. Survival results were analyzed by the Kaplan–Meier technique using GraphPad Prism software. A log-rank test for comparisons was used. \**P* < 0.05 was considered significant, and \*\**P* < 0.01 \*\*\**P* < 0.001 were considered highly significant.

## Supporting Information

Supporting Information is available from the Wiley Online Library or from the author.

## Acknowledgements

This work was supported by the National Natural Science Foundation of China (NSFC 51773145, 51473110, 51633005, and 51761135117).

## Conflict of Interest

The authors declare no conflict of interest.

## Keywords

cancer therapy, polymersomes, polypeptides, small interfering RNA (siRNA), targeted delivery

Received: April 17, 2019

Revised: May 31, 2019

Published online:

- [1] a) S. Y. Wu, G. Lopez-Berestein, G. A. Calin, A. K. Sood, *Sci. Transl. Med.* **2014**, *6*, 240ps7; b) M. L. Bobbin, J. J. Rossi, *Annu. Rev. Pharmacol. Toxicol.* **2016**, *56*, 103; c) G. Ozcan, B. Ozpolat, R. L. Coleman, A. K. Sood, G. Lopez-Berestein, *Adv. Drug Delivery Rev.* **2015**, *87*, 108; d) J. E. Zuckerman, M. E. Davis, *Nat. Rev. Drug Discovery* **2015**, *14*, 843.
- [2] a) A. B. Hi, M. Chen, C.-K. Chen, B. A. Pfeifer, C. H. Jones, *Trends Biotechnol.* **2016**, *34*, 91; b) T. Wang, S. Shigdar, H. Al Shamaileh, M. P. Gantier, W. Yin, D. Xiang, L. Wang, S.-F. Zhou, Y. Hou, P. Wang, W. Zhang, C. Pu, W. Duan, *Cancer Lett.* **2017**, *387*, 77; c) H. J. Kim, A. Kim, K. Miyata, K. Kataoka, *Adv. Drug Delivery Rev.* **2016**, *104*, 61; d) M. W. Amjad, P. Kesharwani, M. C. I. M. Amin, A. K. Iyer, *Prog. Polym. Sci.* **2017**, *64*, 154.
- [3] a) U. Laechelt, E. Wagner, *Chem. Rev.* **2015**, *115*, 11043; b) Z. Zhou, X. Liu, D. Zhu, Y. Wang, Z. Zhang, X. Zhou, N. Qiu, X. Chen, Y. Shen, *Adv. Drug Delivery Rev.* **2017**, *115*, 115; c) X. Xu, J. Wu, Y. Liu, P. E. Saw, W. Tao, M. Yu, H. Zope, M. Si, A. Victorious, J. Rasmussen, D. Ayyash, O. C. Farokhzad, J. Shi, *ACS Nano* **2017**, *11*, 2618; d) C. Xu, P. Wang, J. Zhang, H. Tian, K. Park, X. Chen, *Small* **2015**, *11*, 4321.
- [4] a) S. Rietwyk, D. Peer, *ACS Nano* **2017**, *11*, 7572; b) L. Huang, Y. Liu, *Annu. Rev. Biomed. Eng.* **2011**, *13*, 507; c) P. M. Klein, S. Kern,

- D.-J. Lee, J. Schmaus, M. Hohn, J. Gorges, U. Kazmaier, E. Wagner, *Biomaterials* **2018**, *178*, 630; d) S. He, W. Fan, N. Wu, J. Zhu, Y. Miao, X. Miao, F. Li, X. Zhang, Y. Gan, *Nano Lett.* **2018**, *18*, 2411.
- [5] a) W. Tai, X. Gao, *Adv. Drug Delivery Rev.* **2017**, *110–111*, 157; b) W. Li, D. Wang, X. Shi, J. Li, Y. Ma, Y. Wang, T. Li, J. Zhang, R. Zhao, Z. Yu, F. Yin, Z. Li, *Mater. Horiz.* **2018**, *5*, 745.
- [6] J. Conde, A. Ambrosone, Y. Hernandez, F. Tian, M. McCully, C. C. Berry, P. V. Baptista, C. Tortiglione, J. M. de la Fuente, *Nano Today* **2015**, *10*, 421.
- [7] J. Shen, W. Zhang, R. Qi, Z.-W. Mao, H. Shen, *Chem. Soc. Rev.* **2018**, *47*, 1969.
- [8] a) H. Cabral, K. Miyata, K. Osada, K. Kataoka, *Chem. Rev.* **2018**, *118*, 6844; b) Z. Song, Z. Han, S. Lv, C. Chen, L. Chen, L. Yin, J. Cheng, *Chem. Soc. Rev.* **2017**, *46*, 6570; c) T. J. Deming, *Wiley Interdiscip. Rev.: Nanomed. Nanobiotechnol.* **2014**, *6*, 283; d) C. Deng, J. Wu, R. Cheng, F. Meng, H.-A. Klok, Z. Zhong, *Prog. Polym. Sci.* **2014**, *39*, 330; e) C. He, X. Zhuang, Z. Tang, H. Tian, X. Chen, *Adv. Healthcare Mater.* **2012**, *1*, 48.
- [9] a) R. J. Christie, Y. Matsumoto, K. Miyata, T. Nomoto, S. Fukushima, K. Osada, J. Halnaut, F. Pittella, H. J. Kim, N. Nishiyama, K. Kataoka, *ACS Nano* **2012**, *6*, 5174; b) Y. Oe, R. J. Christie, M. Naito, S. A. Low, S. Fukushima, K. Toh, Y. Miura, Y. Matsumoto, N. Nishiyama, K. Miyata, K. Kataoka, *Biomaterials* **2014**, *35*, 7887; c) H. J. Kim, T. Ishii, M. Zheng, S. Watanabe, K. Toh, Y. Matsumoto, N. Nishiyama, K. Miyata, K. Kataoka, *Drug Delivery Transl. Res.* **2014**, *4*, 50; d) H. Nishida, Y. Matsumoto, K. Kawana, R. J. Christie, M. Naito, B. S. Kim, K. Toh, H. S. Min, Y. Yi, Y. Matsumoto, H. J. Kim, K. Miyata, A. Taguchi, K. Tomio, A. Yamashita, T. Inoue, H. Nakamura, A. Fujimoto, M. Sato, M. Yoshida, K. Adachi, T. Arimoto, O. Wada-Hiraike, K. Oda, T. Nagamatsu, N. Nishiyama, K. Kataoka, Y. Osuga, T. Fujii, *J. Controlled Release* **2016**, *231*, 29.
- [10] a) H. J. Kim, K. Miyata, T. Nomoto, M. Zheng, A. Kim, X. Liu, H. Cabral, R. J. Christie, N. Nishiyama, K. Kataoka, *Biomaterials* **2014**, *35*, 4548; b) C. Zheng, M. Zheng, P. Gong, J. Deng, H. Yi, P. Zhang, Y. Zhang, P. Liu, Y. Ma, L. Cai, *Biomaterials* **2013**, *34*, 3431.
- [11] S. Florinas, M. Liu, R. Fleming, L. Van Vlerken-Ysla, J. Ayriss, R. Gilbreth, N. Dimasi, C. Gao, H. Wu, Z.-Q. Xu, S. Chen, A. Dirisala, K. Kataoka, H. Cabral, R. J. Christie, *Biomacromolecules* **2016**, *17*, 1818.
- [12] a) H. He, N. Zheng, Z. Song, K. H. Kim, C. Yao, R. Zhang, C. Zhang, Y. Huang, F. M. Uckun, J. Cheng, Y. Zhang, L. Yin, *ACS Nano* **2016**, *10*, 1859; b) N. Zheng, Z. Song, Y. Liu, R. Zhang, R. Zhang, C. Yao, F. M. Uckun, L. Yin, J. Cheng, *J. Controlled Release* **2015**, *205*, 231.
- [13] a) H. J. Kim, Y. Yi, A. Kim, K. Miyata, *Biomacromolecules* **2018**, *19*, 2377; b) F. Li, Y. Li, Z. Zhou, S. Lv, Q. Deng, X. Xu, L. Yin, *ACS Appl. Mater. Interfaces* **2017**, *9*, 23586.
- [14] H. Hatakeyama, H. Akita, H. Harashima, *Adv. Drug Delivery Rev.* **2011**, *63*, 152.
- [15] a) F. Meng, Z. Zhong, J. Feijen, *Biomacromolecules* **2009**, *10*, 197; b) H. De Oliveira, J. Thevenot, S. Lecommandoux, *Wiley Interdiscip. Rev.: Nanomed. Nanobiotechnol.* **2012**, *4*, 525; c) Y. Zhu, B. Yang, S. Chen, J. Du, *Prog. Polym. Sci.* **2017**, *64*, 1; d) X. Hu, Y. Zhang, Z. Xie, X. Jing, A. Bellotti, Z. Gu, *Biomacromolecules* **2017**, *18*, 649; e) Y. Zou, M. Zheng, W. Yang, F. Meng, K. Miyata, H. J. Kim, K. Kataoka, Z. Zhong, *Adv. Mater.* **2017**, *29*, 1703285.
- [16] a) A. P. Pandey, K. K. Sawant, *Mater. Sci. Eng., C* **2016**, *68*, 904; b) Y. S. Malik, M. A. Sheikh, Z. Xing, Z. Guo, X. Zhu, H. Tian, X. Chen, *Acta Biomater.* **2018**, *80*, 144.
- [17] a) M. Qiu, J. Ouyang, H. Sun, F. Meng, R. Cheng, J. Zhang, L. Cheng, Q. Lan, C. Deng, Z. Zhong, *ACS Appl. Mater. Interfaces* **2017**, *9*, 27587; b) M. Qiu, Z. Zhang, Y. Wei, H. Sun, F. Meng, C. Deng, Z. Zhong, *Chem. Mater.* **2018**, *30*, 6831.
- [18] a) E. Kondo, K. Saito, Y. Tashiro, K. Kamide, S. Uno, T. Furuya, M. Mashita, K. Nakajima, T. Tsumuraya, N. Kobayashi, M. Nishibori, M. Tanimoto, M. Matsushita, *Nat. Commun.* **2012**, *3*, 951; b) W. Yang, Y. Xia, Y. Fang, F. Meng, J. Zhang, R. Cheng, C. Deng, Z. Zhong, *Adv. Healthcare Mater.* **2017**, 1701135; c) T. Lin, E. Liu, H. He, M. C. Shin, C. Moon, V. C. Yang, Y. Huang, *Acta Pharm. Sin. B* **2016**, *6*, 352.
- [19] a) X. Q. Liu, R. L. Erikson, *Proc. Natl. Acad. Sci. USA* **2003**, *100*, 5789; b) K. Strebhardt, A. Ullrich, *Nat. Rev. Cancer* **2006**, *6*, 321.
- [20] Y.-D. Yao, T.-M. Sun, S.-Y. Huang, S. Dou, L. Lin, J.-N. Chen, J.-B. Ruan, C.-Q. Mao, F.-Y. Yu, M.-S. Zeng, J.-Y. Zang, Q. Liu, F.-X. Su, P. Zhang, J. Lieberman, J. Wang, E. Song, *Sci. Transl. Med.* **2012**, *4*, 130ra48.
- [21] N. Graf, D. R. Bielenberg, N. Kolishetti, C. Muus, J. Banyard, O. C. Farokhzad, S. J. Lippard, *ACS Nano* **2012**, *6*, 4530.
- [22] H. Gao, Q. Zhang, Y. Yang, X. Jiang, Q. He, *Int. J. Pharm.* **2015**, *478*, 240.
- [23] J. Gilleron, W. Querbes, A. Zeigerer, A. Borodovsky, G. Marsico, U. Schubert, K. Manygoats, S. Seifert, C. Andree, M. Stoeter, H. Epstein-Barash, L. Zhang, V. Kotliansky, K. Fitzgerald, E. Fava, M. Bickle, Y. Kalaidzidis, A. Akinc, M. Maier, M. Zerial, *Nat. Biotechnol.* **2013**, *31*, 638.
- [24] a) J. E. Zuckerman, I. Gritli, A. Tolcher, J. D. Heidel, D. Lim, R. Morgan, B. Chmielowski, A. Ribas, M. E. Davis, Y. Yen, *Proc. Natl. Acad. Sci. USA* **2014**, *111*, 11449; b) B. Naeye, H. Deschout, V. Cavelliers, B. Descamps, K. Braeckmans, C. Vanhove, J. Demeester, T. Lahoutte, S. C. De Smedt, K. Raemdonck, *Biomaterials* **2013**, *34*, 2350.
- [25] a) Y.-N. Zhang, W. Poon, A. J. Tavares, I. D. McGilvray, W. C. W. Chan, *J. Controlled Release* **2016**, *240*, 332; b) W. Cheng, J. Nie, N. Gao, G. Liu, W. Tao, X. Xiao, L. Jiang, Z. Liu, X. Zeng, L. Mei, *Adv. Funct. Mater.* **2017**, *27*; c) X. Zeng, M. Luo, G. Liu, X. Wang, W. Tao, Y. Lin, X. Ji, L. Nie, L. Mei, *Adv. Sci.* **2018**, *5*, 1800510.
- [26] M. Qiu, H. L. Sun, F. H. Meng, R. Cheng, J. Zhang, C. Deng, Z. Y. Zhong, *J. Controlled Release* **2018**, *272*, 107.